Available online at www.sciencedirect.com

ScienceDirect

Ceramics International 37 (2011) 431–435

CERAMICS INTERNATIONAL

www.elsevier.com/locate/ceramint

Short communication

On some properties of PZT–NZF composite films manufactured by hybrid synthesis route

K.P. Pramoda, A. Huang, S.R. Shannigrahi *

*Institute of Materials Research and Engineering, A*STAR (Agency for Science, Technology and Research), 3 Research Link, Singapore 117602, Singapore*

Received 18 February 2010; received in revised form 26 June 2010; accepted 1 September 2010
Available online 1 October 2010

Abstract

Composite magnetoelectric films using ferroelectric lead zirconate titanate (PZT) and ferromagnetic nickel zinc ferrite (NZF) were prepared using the combination of sol–gel and hydrothermal process on $Pt/Ti/SiO_2/Si$ substrates. The thickness was estimated ~2 μm using cross-sectional SEM. Structure, morphology and electro-magnetic characterization were assessed using XRD, XPS, SEM, dielectric, leakage current, ferroelectric, and magnetic property analyze. The composite films exhibit coexistence of ferroelectric and ferromagnetic ordering at room temperature with a remnant polarization (P_r), and coercive field (E_c) of 1.2 μC/cm^2 and 7.8 kV/cm, respectively, and saturation magnetization (M_s) ~20 emu/cm^3. Polarization improved ~5.2% upon poling the composite film using a magnetic field of 1 T.

Keywords: Multiferroics; PZT; (PZT–NZF) film composition and structure; XPS; SEM

1. Introduction

Below a characteristic temperature the spontaneous magnetization and polarization of magnetoelectric (ME) materials can be switched by an applied electric or a magnetic field, respectively. There also exists some coupling between their piezo and magnetostrictive properties, which make ME materials extremely attractive for new generation devices like sensors, memory, transducers, actuators, etc. [1–4]. Among the ME materials, $BiFeO_3$, $BiMnO_3$, etc., appear as single phase ME materials, which mostly exhibit weak coupling and are not suitable for device applications [5,6]. As an alternative, composites, which incorporate ferroelectric and ferri-/ferromagnetic phases, typically yield higher ME coupling response [7–9] defined as follows:

$$\text{ME effect} = \frac{\text{electrical}}{\text{mechanical}} \times \frac{\text{mechanical}}{\text{magnetic}} \quad (1)$$

The strain mediated coupling decreases rapidly with miniaturization. So, to realize micro/nano-devices using composites, it is required to prepared thick film (2–5 μm). However, it is difficult to prepare crack-free films thicker than 1 μm by sol–gel conventional method. As this method has the limitation for crack free film thickness of ~400 nm beyond which cracks generally appear on the film surface due to mechanical stress during annealing. Up to now there are only a few investigations available on the thick ME films [10–14].

For composite ME materials preparation individual components should have high piezoelectric and magnetic properties, keeping this in view, one of the most preferred choices should be PZT and NiZn-ferrites as the PZT is considered one of the best piezoelectric materials similarly NZF shows quite good magnetic properties [15–19]. This study reports the microstructure, dielectric, ferroelectric, magnetic, and multiferroic properties of $Pb(Zr_{0.52}Ti_{0.48})O_3–Ni_{0.50}Zn_{0.50}Fe_2O_4$ (PZT–NZF) composite films prepared by sol–gel and hydrothermal based hybrid process.

2. Experiments

The PZT films were prepared using sol–gel spin coating technique on $Pt/Ti/SiO_2/Si$ substrates. Details of the PZT preparation were given elsewhere [20]. To produce PZT–NZF composite films, the PZT film (thickness 0.8 μm) was first deposited as under layer for developing NZF film on it.

* Corresponding author. Fax: +65 68720785.
E-mail address: santi-s@imre.a-star.edu.sg (S.R. Shannigrahi).

0272-8842/$36.00
doi:10.1016/j.ceramint.2010.09.029

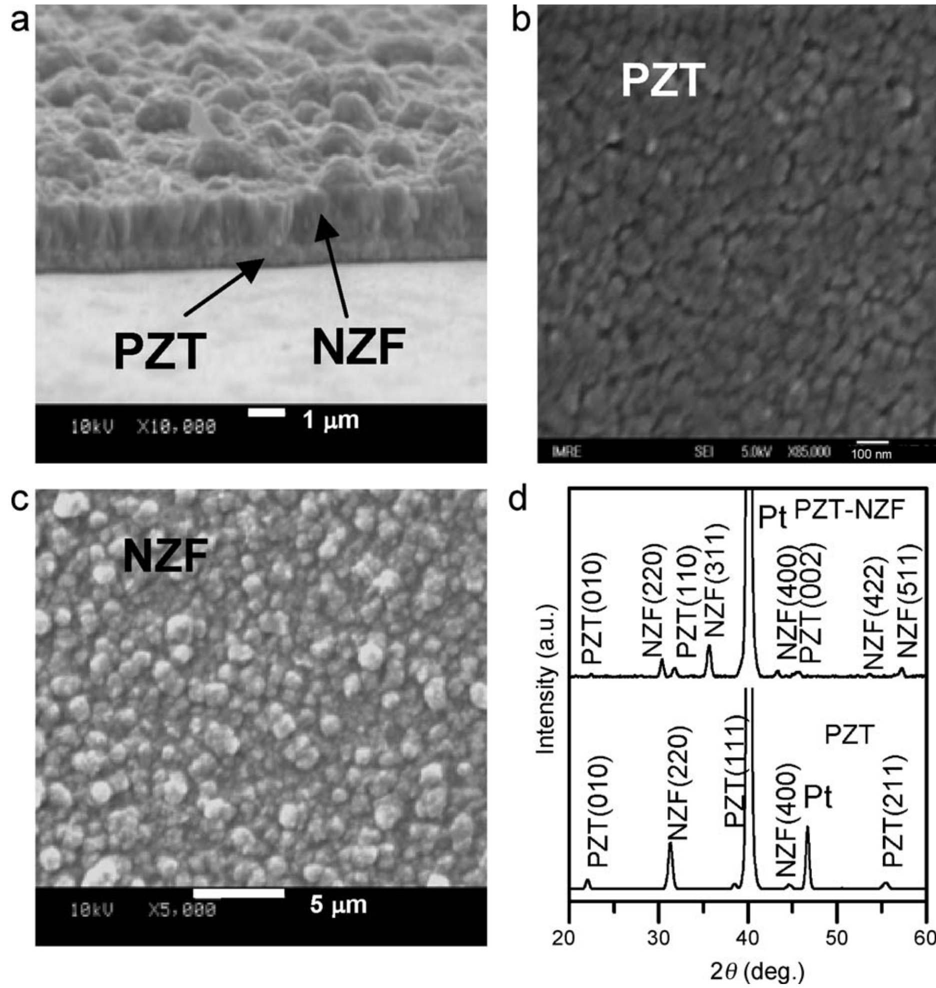

Fig. 1. (a) Cross-section of the PZT–NZF composite films, (b) and (c) the surface morphology of PZT and NZF films, respectively, and (d) the XRD patterns.

The NZF films (thickness 1.2 μm) were manufactured by the hydrothermal technique. The detailed film manufacturing procedure was given elsewhere [21]. The crystallinity was investigated by X-ray-diffraction (XRD) with Cu Kα radiation in the Bragg angle range of ($10^\circ \leq 2\theta \leq 60^\circ$). The layer surface morphology and thickness were assessed by field emission gun scanning electron microscopy (FE-SEM) (JSM-6700F, JEOL Ltd., Japan). A vibrating sample magnetometer (VSM) system (Lake Shore 7400) was used for measuring the field dependence magnetization of the samples. The correction for the diamagnetic contributions from the substrate and PZT was applied. For electrical characterization, gold was sputtered deposited through a shadow mask to get round electrodes of 0.2 mm diameter and thickness of 10 nm. *P–E* hysteresis loop measurement was carried out using a standard ferroelectric testing unit RT66A. The room temperature leakage current property of the films was measured using an electrometer system (Agilent 4156B). Dielectric constant and loss were measured using an impedance analyzer (HP4194A). The surface chemistry of the film was studied with X-ray photoelectron spectroscopy (XPS) (VG) ESCALAB 2201-XL Imaging System, England). XPS profiles of the samples were obtained using Al Kα source (1486.6 eV).

3. Results and discussion

Fig. 1(a)–(c) displays the typical SEM cross-sections, and surface morphologies of the films. The thickness was estimated to be ~2 μm with PZT and NZF thicknesses are 0.8 μm and 1.2 μm, respectively. The surface is crack-free with a granular structure without any pore. The NZF particles with average diameter of ~60 nm are uniformly distributed in the PZT matrix. Fig. 1(d) depicts the XRD patterns of the perovskite PZT and the PZT–NZF composite films. The peaks of the PZT and PZT–NZF films are indexed according to the JCPDS files numbers 73-2022 and 08-0234, respectively. The XRD pattern indicates that the composite film consists of two separate perovskite PZT and spinel NZF phases. No chemical reaction or phase diffusion are observed between the NZF and PZT phases. In addition, both phases exhibit polycrystalline structures.

Fig. 2(a) shows the *P–E* hysteresis cycle of the composite films at room temperature. Saturation of polarization was not obtained even at high electric field values. The remnant polarization (P_r) and coercive field (E_c), of the composite film were ~1.2 μC/cm^2 and ~7.8 kV/cm, respectively, at an applied maximum electric field of 30 kV/cm. The saturated or maximum polarization (P_s) of the composite film was found to be ~3.5 μC/cm^2, which is low value compared to PZT film

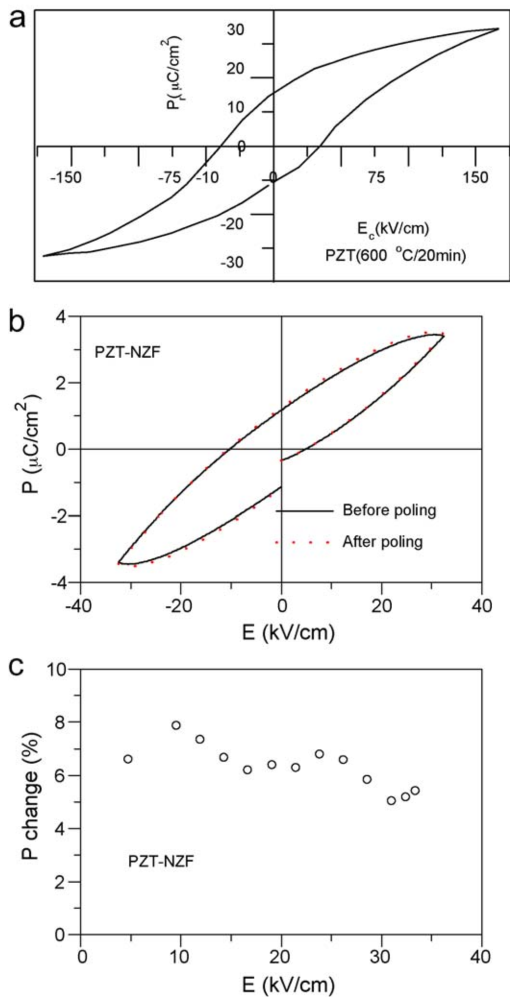

Fig. 2. (a) *P–E* hysteresis loop of PZT film. (b) and (c) depict the *P–E* hysteresis loops of the PZT–NZF composite films with and without magnetic field of 1 T and the percentage polarization change across applied electric field for the PZT–NZF films poled with magnetic field of 1 T.

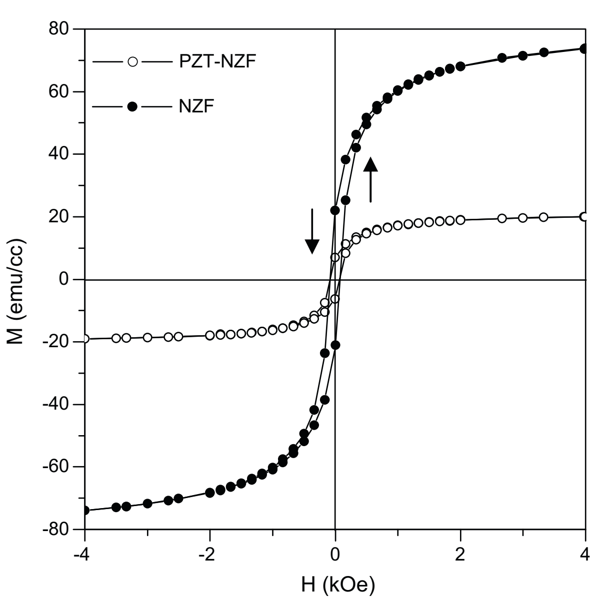

Fig. 3. *M–H* hysteresis loops of the PZT–NZF composite films.

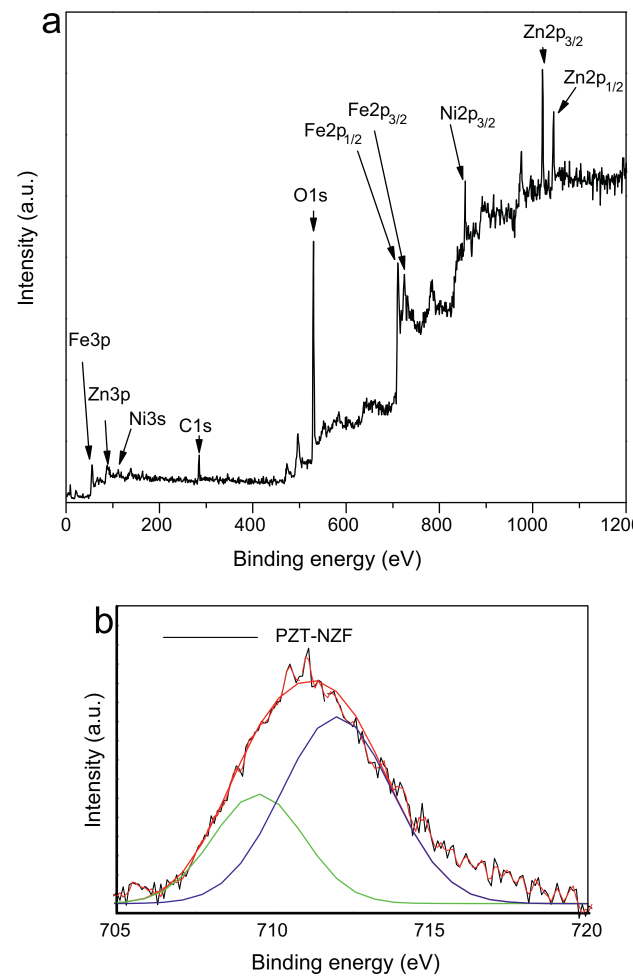

Fig. 4. (a) Shows the XPS wide range spectrum analysis and (b) the XPS spectra of Fe 2p line for the PZT–NZF composite films.

itself, as depicted in Fig. 2(a). This is probably due to the dead layer between the PZT and the NZF, which exist and results pinning effect on the NZF film [9]. It is very likely that the NZF might make the films hard to pole as they are on the PZT layer and act as grain boundary pinning of the ferroelectric domains. When the NiZn content has equal amount, the *P–E* loop exhibits a similar polarization loop with reduced P_r. The variation of the ferroelectric polarization under applied magnetic field was characterized. The films were poled using a magnetic field of 1 T for an hour before the ferroelectric polarizations were measured. It is observed that the magnetic field poling of 1 T caused an improvement in the polarization values of the composite film by about 5% as shown in Fig. 2(c). Such results clearly demonstrate the multiferroic behavior of the composite films [22].

The composite film exhibits a well-defined *M–H* magnetic hysteresis loop (Fig. 3). The saturation magnetization (M_s) and coercive field (H_c) are 20 emu/cm^3 and 70 Oe, respectively. The M_s value for the present composite film is slightly higher than that of the pure $Ni_{0.5}Zn_{0.5}Fe_2O_4$ film while it exhibits a comparable H_c value. The observed higher value of M_s is possibly attributed to the large residual stress in $Ni_{0.5}Zn_{0.5-}$

Fe_2O_4 due to the lattice mismatch and coefficient of thermal expansion (CTE) difference between the PZT (~(3–5) × 10^{-6}/°C) and NZF (~(8–10) × 10^{-6}/°C) phases. This easy magnetization characteristic is beneficial to the enhancement of magnetoelectric coupling between the ferroelectric and ferromagnetic phases at low magnetic field.

The Fe oxidation state of the surface of the composite film was investigated using XPS. The wide scan XPS spectra as shown in Fig. 4(a) suggested that there are no impurities present in the film. A representative scan of the Fe 2p line is shown in Fig. 4(b). The position of this line is expected to be 711.6 eV for Fe^{3+} and 709.5 eV for Fe^{2+}, and the position of the satellite is expected at 719 eV for Fe^{3+} and 716 eV for Fe^{2+}. Peak fitting demonstrates that the oxidation state of Fe in the ferrite films is the coexistence of both Fe^{3+} and Fe^{2+} with a ratio of about 65:35. In general, magnetite contains 2/3 Fe^{3+} ions and 1/3 Fe^{2+} ions leading to broader Fe 2p signals in the XPS spectrum. Therefore, it reveals that iron retains its valance state irrespective of changes in its chemical environment. Hence there is no chemical reaction among the two phases of PZT and NZF. The coexistence of both Fe^{3+} and Fe^{2+} would hence contribute to the ferromagnetism of the composite film. Ni $2p_{3/2}$, Zn $2p_{3/2}$ and O 1s exhibited binding energy values of 855, 1021.7 and 530 eV, respectively. This clearly indicates that the Fe, Ni, Zn elements retain their oxidation states of 3+, 2+ and 2+, respectively.

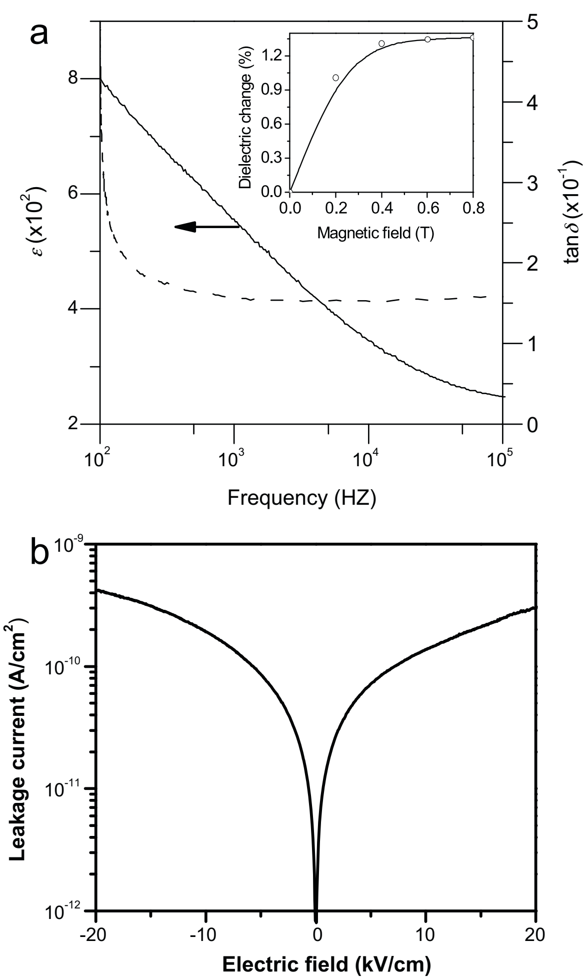

Fig. 5. (a) Variation of dielectric constant and loss with frequency. Inset shows the variation of dielectric constant with magnetic field for the PZT–NZF composite films. (b) Leakage current behavior at room temperature.

Fig. 5(a) demonstrates the frequency variation of dielectric properties of the composite films. It is observed that with an increase in frequency up to 10^4 Hz, both dielectric and loss decrease which indicates a typical characteristic of normal dielectric materials. The dielectric loss value of the composite film at room temperature was found to be quite high (~0.5). Inset in Fig. 5(a) shows the variation of dielectric constant of the composite thin films with an applied magnetic field up to 0.8 T [22].

Fig. 5b shows current density versus electric field (J–E) characteristics of the composite film measured at room temperature (RT). It can be seen that there is no difference between forward and reverse bias conditions of the leakage current and also absence of any break down characteristics of the film. The lowest leakage current density obtained was about 10^{-10} A/cm^2 at 5 kV/cm for the as deposited film without any heat treatment process. This is consistent with observations from XPS. Low Fe^{2+} content implies very likely less oxygen vacancy which accounts for the lower leakage current.

4. Conclusions

Composite (PZT–NZF) thick films (thickness 2 μm) were manufactured using the combination of sol–gel and hydrothermal hybrid processing routes. This hybrid process results in crack free homogeneous and dense thick films. The XRD pattern indicates that the composite film consists of two separate phases of the perovskite PZT and spinel NZF. No chemical reaction or phase diffusion is observed between the NZF and PZT phases. In addition, both phases exhibit polycrystalline structures. The composite film exhibits coexistence of ferroelectric and ferromagnetic ordering at room temperature with P_s ~2 μC/cm^2 and M_s ~20 emu/cm^3. Ferroelectric polarization improvements about 5% were observed by poling the composite films with a magnetic filed of 1 T. This clearly indicates the multiferroic property in the composite films at room temperature.

References

[1] R. McCurrie, Ferromagnetic Materials, Structure and Properties, Academic Press, London, 1994, pp. 132–158.
[2] H.M. Pardavi, J. Magn. Magn. Mater. 171 (2000) 215.
[3] S. Komarneni, E. Fregeau, E. Breval, R. Roy, J. Am. Ceram. Soc. 71 (1998) C26.
[4] A.S. Albuquerque, J.D. Ardisson, W.A.A. Macedoet, J. Magn. Magn. Mater. 192 (1999) 277.
[5] S. Son, M. Taheri, E. Carpenter, V.G. Harris, M.E. McHenry, J. Appl. Phys. 91 (2002) 7589.
[6] G. Srinivasan, V.M. Laletsin, R. Hayes, N. Puddubnaya, E.T. Rasmussen, D.J. Fekel, Solid State Commun. 124 (2002) 373.
[7] J.G. Wan, H. Zhang, X.W. Wang, D.Y. Pan, J.M. Liu, G.H. Wang, Appl. Phys. Lett. 89 (2006) 122914.
[8] J. Ryu, A.V.Z. Carazo, K. Uchino, H.E. Kim, J. Electroceram. 7 (2001) 17.

[9] J. Wang, J.B. Neaton, H. Zheng, V. Nagarajan, S.B. Ogale, B. Liu, D. Viehland, V. Vaithyanathan, D.G. Schlom, U.V. Waghmare, N.A. Spaldin, K.M. Rabe, M. Wuttig, R. Ramesh, Science 299 (2003) 1719.
[10] C.S. Park, J. Ryu, J.J. Choi, D.S. Park, C.W. Ahn, S. Priya, Jpn. J. Appl. Phys. 48 (2009) 080204.
[11] D.A. Filippov, G. Srinivasan, A. Gupta, J. Phys. Condens. Matter 20 (2008) 425306.
[12] S. Ryu, J.H. park, H.M. Jang, Appl. Phys. Lett. 91 (2007) 142910.
[13] MaF Y.G., W.N. Cheng, M. Ning, C.K. Ong, Appl. Phys. Lett. 90 (2007) 152911.
[14] G. Srinivasan, E.T. Rasmussen, R. Hayes, Phys. Rev. 67 (2003) 014418.
[15] A.A. Bush, V.Y. Shkuratov, I.A. Chernykh, Y.K. Fetisov, Tech. Phys. 55 (2010) 387.
[16] A.S. Tatarenko, V. Gheevarughese, G. Srinivasan, O.V. Antonenkov, M.I. Bichurin, J. Electroceram. 24 (2010) 5.
[17] A.K. Yang, C.A. Wang, R. Guo, Y. Huang, C.W. Nan, Ceram. Int. 36 (2010) 549.
[18] C. Galassi, J. Eur. Ceram. Soc. 26 (2006) 2951.
[19] S. Miroslav, M. Vlastimil, G. Tomá, K. Jana, Ceram. Int. 26 (2000) 507.
[20] S.R. Shannigrahi, S.H. Lee, H.M. Jang, J. Am. Ceram. Soc. 85 (2002) 2122.
[21] K.P. Pramoda, T.S. Mun, G.K.L. Goh, B.K. Lok, A. Lu, J. Nanosci. Nanotech. 8 (2008) 2609.
[22] S.Y. Tan, S.R. Shannigrahi, S.H. Tan, F.E.H. Tay, J. Appl. Phys. 103 (2008) 094105.